

CHAPTER ONE HUNDRED FORTY EIGHT

Modeling of Nearshore Wave Driven Currents

Jon M. Hubertz¹

Abstract

A nearshore current modeling system has been assembled which consists of a shallow water directional spectral wave model, an algorithm to convert directional spectral output from the wave model to radiation stress components and a current model to calculate nearshore wave-driven currents from the radiation stress field.

Wave-driven longshore currents have been hindcast at a coastal site for two wave conditions during a northeaster type storm off Cape Hatteras in October 1982. For one event, when local winds were strong, the calculated longshore current is only a fraction of what was measured. This discrepancy is attributed to a non-wave-driven component of flow which was present but not represented in the model. During the other event, winds were low and long period swell was present. In this case, the calculated and measured longshore flow agree well.

Both measured and calculated shore normal profiles of longshore current in each case show a generally uniform structure across the surf zone. This is in contrast to theoretical profiles based on monochromatic waves which show a maximum in longshore flow near the breaker line.

Introduction

The U. S. Army Engineer Waterways Experiment Station, Coastal Engineering Research Center (CERC) is sponsoring research to improve our capability to predict currents in the nearshore area. The prediction techniques which result from this program will then be available to support studies of sediment transport. A workshop held in the summer of 1982 on the subject of modeling nearshore currents provided a forum for discussion of what improvements are most needed to improve nearshore current models. One conclusion of the workshop attendees was that to predict wave-driven currents improvements were needed in transformation of the wave field from the input boundary of a model to the shoreline. It was concluded that acceptable predictions of wave-driven currents were possible only if the distribution of wave parameters in the model region was correct. We have concentrated recently on improving our ability to predict nearshore wave conditions.

Recent research on the transformation of shallow water wave spectra (2) has provided a promising technique to obtain nearshore wave

¹Research Division, Coastal Engineering Research Center, U. S. Army Engineer Waterways Experiment Station, P. O. Box 631, Vicksburg, MS 39180

conditions. This technique has been incorporated in a two-dimensional directional spectral wave model. Output of the model is a directional spectrum at each grid point over the model region. Each spectrum is a function of wave angle, frequency and depth. These spectra are integrated over frequency and direction to provide an estimate of the three components of radiation stress at each grid point. This field of radiation stress components provides the driving force in a circulation model to predict longshore and cross-shore flows. The wave, radiation stress and current calculations are assembled as a nearshore current modeling system.

Field measurements at CERC's Field Research Facility (FRF) were made in cooperation with the United States Geological Survey (USGS) in the fall of 1982. They provide estimates of longshore and cross-shore flows as well as wave heights along a line normal to shore through the surf zone. Data sets such as these are quite valuable in studying nearshore processes and evaluating models. However, such data may contain the effects of a number of forcing functions such as waves, tides, winds, current fronts, etc. This makes it difficult to isolate particular components for individual study and for comparison to model results where all the processes in nature are not included. Each component in the modeling system is discussed in more detail below, as well as the field measurements and some model results.

Nearshore Current Modeling System

Shallow Water Spectral Wave Model.-The basis for the wave model is the model developed by Hsiao (5) to investigate wave energy dissipation in shallow water due to bottom effects. It computes over two horizontal dimensions and allows two-dimensional variation of depth. It is a steady state model which considers the balance of spectral energy among terms for advection of wave energy, refraction and shoaling effects, atmospheric input, bottom friction, percolation and nonlinear wave interactions. The wave number spectral balance equation of the model is:

$$\frac{\partial F(\bar{k}, \bar{x}, t)}{\partial x_i} \frac{dx_i}{dt} = S_A + S_N + S_F + S_P$$

where $F(\bar{k}, \bar{x}, t)$ is the wave number spectrum and the lefthand side represents refraction and shoaling effects and the righthand side, source terms S_A - atmospheric input, S_N - nonlinear wave interaction, S_F - bottom friction and S_P - percolation. In addition to these terms, a modification to the model has been made to limit the spectral energy in shallow water by imposing a spectral shape called the TEXEL, MARSEN, ARSLOE (TMA) spectrum. This spectrum provides a favorable fit to about 2800 measured spectra from the three field experiments above. It is related to a quasi-equilibrium deep water spectral shape called the JONSWAP spectrum, (4) by the factor ϕ which results in a quasi-equilibrium shallow water spectral shape. The ϕ factor, (6) varies between zero and one as a function of nondimensional frequency W_h where $W_h = 2\pi f \left(\frac{h}{g}\right)^{1/2}$ and h is depth, g gravity, and f is frequency.

A value of zero refers to zero depth and one to deep water. Thus the TMA spectrum can be expressed as:

$$E_{TMA}(f, h) = E_{JSWP}(f) \phi(f, h)$$

with JONSWAP parameters determined from the TMA shallow water data set.

This spectrum appears to account for the distribution of spectral energy in shallow water and with a minor correction even through the surf zone (Vincent, personnel communication). It is not understood at present what physical mechanisms it reflects, only that it approximates the wave spectrum nearshore. If one accepts this, it provides a method to specify spectral energy nearshore and through the surf zone. Thus one no longer has to rely on a monochromatic, single wave direction approach or specify breaking criteria to calculate the distribution of wave energy nearshore.

Calculation of Radiation Stresses

Another conclusion of the Nearshore Currents Workshop mentioned above was that the theory of radiation stress, (7) provides a simple and valid mechanism for the generation of nearshore wave driven currents. According to that theory, to second order for a progressive, linear, small amplitude wave, the radiation stress components are:

$$\begin{aligned} S_{xx} &= E \left[\left(2n - \frac{1}{2} \right) \cos^2 \theta + \left(n - \frac{1}{2} \right) \sin^2 \theta \right], \\ S_{xy} &= E n \cos \theta \sin \theta, \\ S_{yy} &= E \left[\left(2n - \frac{1}{2} \right) \sin^2 \theta + \left(n - \frac{1}{2} \right) \cos^2 \theta \right], \end{aligned}$$

where E is the wave energy density, n the ratio of group velocity to wave celerity and θ the wave angle. Without recourse to an energy distribution, it has been common to express E as

$$E = \frac{1}{8} \rho g H^2$$

where ρ is water density and H is the root mean square wave height. Thus the radiation stress components depend strongly (as the square) on the distribution of wave height and a mean angle. The wave height in the nearshore has generally been taken as more or less constant up to a breaker line where it decreases rapidly with distance to shore. This results in strong gradients in the radiation stress field near the breaker line and hence strong currents and current shears in this area, if θ has some nonzero value (zero indicating waves propagating normal to shore). This approach when combined with some type of lateral eddy viscosity or mixing function to smooth out the velocity field gives comparable results to theory and laboratory observations (1).

In place of the above approach, we have represented the radiation stress components as:

$$S_{xx} = \int_0^{\infty} \int_0^{2\pi} \left[n \cos^2 \theta + \left(n - \frac{1}{2} \right) \right] E(f, \theta) \, d\theta df,$$

$$S_{xy} = \int_0^{\infty} \int_0^{2\pi} (n \sin \theta \cos \theta) E(f, \theta) \, d\theta df,$$

$$S_{yy} = \int_0^{\infty} \int_0^{2\pi} \left[n \sin^2 \theta + \left(n - \frac{1}{2} \right) \right] E(f, \theta) \, d\theta df,$$

where in practice the integrals are replaced by summation of the integrands over the frequency and directional domains and $E(f, \theta, \bar{X})$ is the three-dimensional wave spectrum as a function of position. The three components of radiation stress are calculated at each grid point of the nearshore current model and provide a stress field to generate wave driven currents with a circulation model.

Current Model

The wave driven current model was developed by Vemulakonda (8) and is based on the long wave model of Butler (3). In addition to radiation stress, it includes linear bottom friction, advection and lateral mixing terms. A radiation boundary condition is applied at the offshore boundary to permit transients developed during startup of the numerical solution to propagate out of the grid.

The equations for the conservation of mass and momentum, averaged over time (one wave period) and depth are:

$$\frac{\partial u}{\partial t} + u \frac{\partial u}{\partial x} + v \frac{\partial v}{\partial y} + g \frac{\partial \bar{\eta}}{\partial x} + \frac{1}{\rho d} T_{bx} + \frac{1}{\rho d} \frac{\partial S_{xx}}{\partial x} + \frac{\partial S_{xy}}{\partial y} - \frac{1}{\rho} \frac{\partial T_{xy}}{\partial y} = 0,$$

$$\frac{\partial v}{\partial t} + u \frac{\partial v}{\partial x} + v \frac{\partial v}{\partial y} + g \frac{\partial \bar{\eta}}{\partial y} + \frac{1}{\rho d} T_{by} + \frac{1}{\rho d} \frac{\partial S_{xy}}{\partial x} + \frac{\partial S_{yy}}{\partial y} - \frac{1}{\rho} \frac{\partial T_{xy}}{\partial x} = 0,$$

$$\frac{\partial \bar{\eta}}{\partial t} + \frac{\partial}{\partial x} (ud) + \frac{\partial}{\partial y} (vd) = 0,$$

where u, v are the x, y horizontal components of velocity, $\bar{\eta}$ the mean free surface displacement, d the total depth, T_b bottom friction stress and T_{xy} lateral shear stress. These equations are solved using a three time level, alternating direction, implicit, finite difference scheme. The radiation stress field produced by the directional spectral wave model is input to the current model and held fixed while the current model is stepped to a steady state.

Model Simulation

A set of wave and current observations in the nearshore zone were obtained in the fall of 1982 at CERC's FRF in cooperation with the USGS.

Mean values of wave and current data were provided by the USGS (Sallenger, personnel communication) for comparison with the results from the near-shore current modeling system described above. These data were obtained along a line normal to shore and 457 m north of the FRF pier. The near-shore region modeled and location of wave and current observations in relation to the pier location are shown in Figure 1. Measurements were made with three electromagnetic current meters and a pressure sensor mounted on a sea sled which was pulled to various positions along the profile line shown in Figure 1. The three current meters were mounted 0.54, 0.99, and 1.74 m from the sea bed. Mean values of longshore and cross-shore flow over 34.1 minute intervals were measured at various distances from shore. Estimates of significant wave height were also made using the current data and pressure data independently.

A summary of mean current components and wave heights for measurements made on 10 October 1982 is shown in Figure 2. Early on the morning of 10 October 1982 a northeaster developed in the vicinity of Cape Hatteras. Winds from the northeast reached a sustained maximum of 13 m/sec at the FRF and waves grew to 2.5 m in the direction of the wind by Noon on October 10. Data shown in Figure 2 were collected from 1200 to 2000 hours Eastern Daylight Time (EDT) on 10 October while wind and wave conditions were approximately constant.

The mean longshore flow from the measured values during this period is about 80 cm/sec toward the south and fairly uniform along the shore normal profile out to the last measurement point at 285 m. Wave heights of 2 m were measured at the offshore station on the profile line and heights of 1 m at the station closest to shore. The profile of measured wave heights is shown in Figure 3 along with the wave heights calculated from the spectral model for the existing wind conditions. In the spectral model application, only Miles' mechanism for energy input from the wind and the TMA limiting spectral shape are imposed. The other options, (Phillips' term for energy input due to pressure fluctuations, bottom friction, percolation and nonlinear interactions) are turned off. A bottom profile as shown in Figure 2 is applied uniformly in the along-shore direction. The assumption of uniform alongshore bathymetry is based on the depth contours of Figure 1 in the model region. Both the wave and current model are capable of simulating arbitrary bathymetry. The upper and lower bars on the measurements of significant wave height indicate independent measures of significant height respectively from pressure and current meters on the sled at each station. The measured variation of wave height normal to shore is reproduced well by the spectral model.

Next, the radiation stress components were calculated as described above using the directional spectra at each grid point. The stress components were input to the current model as the only forcing term. The advective terms and the lateral eddy viscosity terms were turned off and the model was time stepped to a steady state. The alongshore current component as measured and calculated is shown in Figure 4. The general trend of both curves is similar although shifted in magnitude by a significant amount.

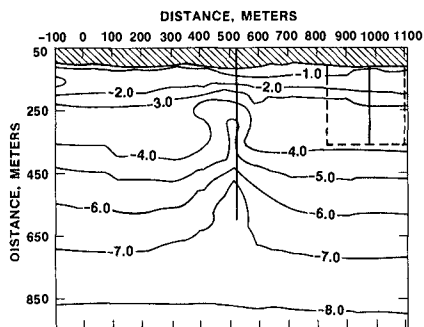


Figure 1. Location of the modeled region (dashed line) in relation to the FRP pier location (solid line over trough). Wave and current observations were made along the solid profile line within the modeled region.

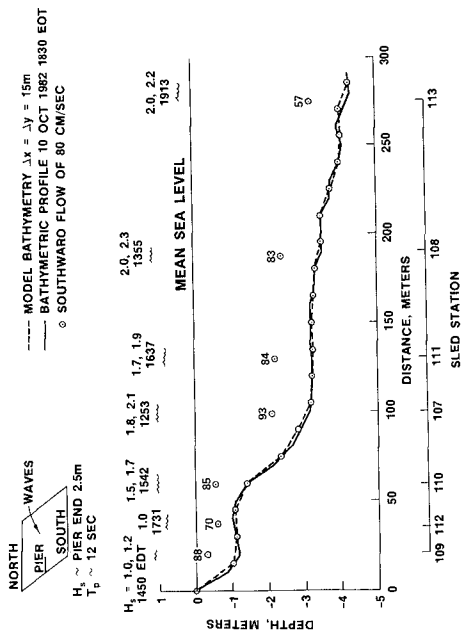


Figure 2. Values of wave height (H_s) derived respectively from current and pressure data at stations along the profile line. The time of observation and water level are indicated below values of H_s . Values of longshore flow shown are averages of values at 0.5, 1.0, 1.75 m above bottom.

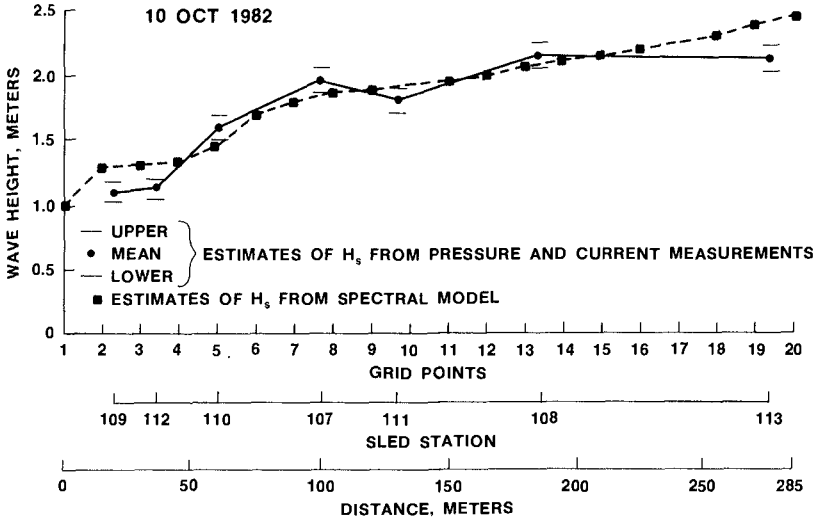


Figure 3. Measured and calculated values of significant wave height along the profile line in the model regions.

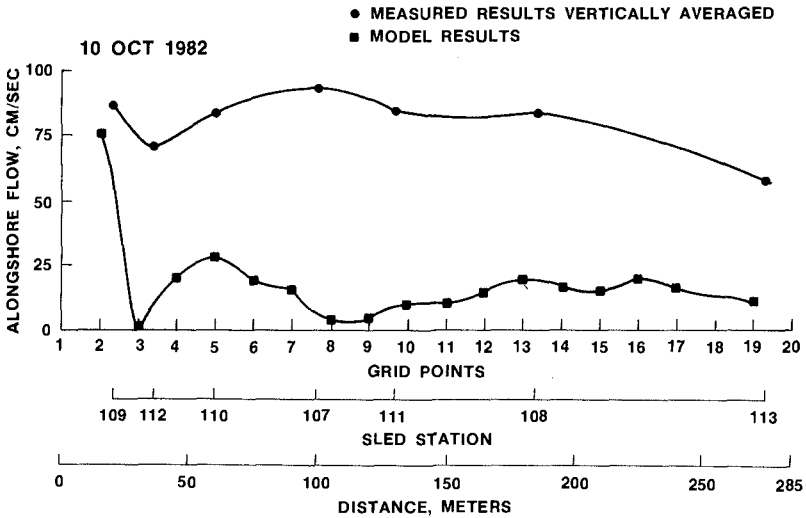


Figure 4. Measured longshore flow and calculated value of the wave-driven component of longshore flow along the profile line in the model region.

Current measurements made from the end of the pier on the morning of 10 October, while the waves were developing, indicate a current toward the south of 55 cm/sec. The surf zone began about 200 m closer to shore than the end of the pier and there was little gradient in wave height near the end of the pier, so this longshore flow was probably not wave induced. There is not enough information to determine the origin of this component of current. A possibility is wind-induced flow. Estimating the surface wind drift as 3 percent of the wind speed would give a value of about 40 cm/sec. If the measured longshore flow in this case is not primarily due to wave driven current, it points out the need to identify and model all of the current generating processes in the nearshore region before one has a generally acceptable nearshore current model.

As this same storm moved offshore, winds at the FRF decreased and large long period waves generated offshore moved toward the pier from the east. On 12 October 1982 waves at the pier end were measured with a significant height of 3 m and peak period of 15 seconds. Such long period waves are extremely unusual on the U. S. East coast. Wave and current measurements were made along the same profile line as on 10 October and are shown in Figure 5. Longshore flow has now shifted northward in response to waves and winds from the southeast quadrant. The average magnitude from the measured values is now about 27 cm/sec. Values are uniform with distance from the shore out to the last measurement station 285 m from shore.

The bathymetric profile has changed from 10 October presumably due to the high wave activity of the previous two days. Figure 6 provides a comparison of the profile changes, showing the bar formation moving deeper and farther offshore.

The spectral wave model was run with the bathymetry appropriate for 12 October 1982. The results are shown in Figure 7. Again, there is good comparison between observed significant wave height and calculated values with a rather uniform decrease in wave height from 2.5 m at the offshore station to 1 m nearshore. The longshore component of flow produced by the current model for this wave height distribution is shown in Figure 8. There is better correlation between measurements and model results in this case leading one to assume that the longshore flow in this case is primarily wave driven.

Note that this longshore flow profile is not typical of theoretical profiles which increase from shore to a maximum inside the "breaker line" and then decrease to zero seaward in a distance about the same as from shore to the "breaker line." The more uniform distribution of longshore flow with distance from shore, as measured and calculated here, is attributed to the uniform decrease in wave height toward shore as observed and modeled in both of the cases considered. The exact physical processes and their relative importance in contributing to the decrease in wave height are unknown. Possibilities would certainly be breaking, white capping, bottom friction and nonlinear interactions. What percentage each of these plays and what other processes are involved remains unknown. It is likely that the key processes will vary

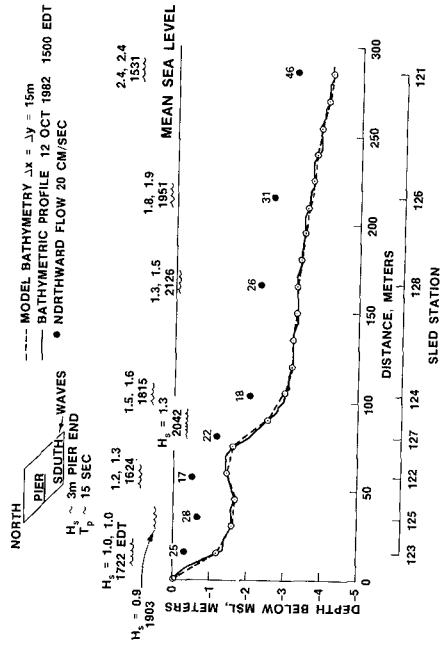


Figure 5. Values of wave height (H_s) derived respectively from current and pressure data at stations along the profile line. The time of observation and water level are indicated below values of H_s . Values of longshore flow shown are averages of values at 0.5, 1.0, 1.75 m above bottom.

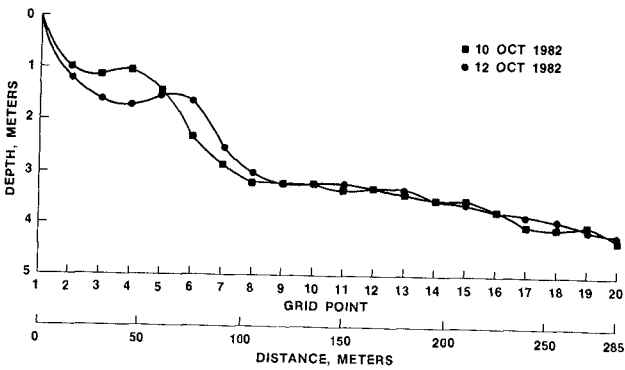


Figure 6. Bathymetric profiles along the profile line in the model.

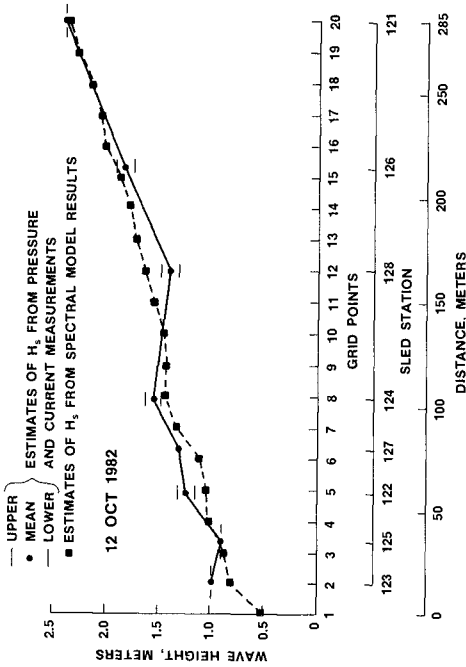


Figure 7. Measured and calculated values of significant wave height along the profile line in the model regions.

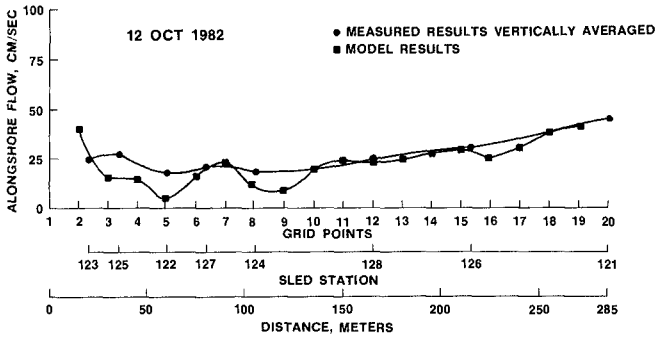


Figure 8. Measured longshore flow and calculated value of the wave-driven component of longshore flow along the profile line in the model region.

for different beach and wave conditions. It is also likely that processes other than wave-driven flow will have to be considered when modeling nearshore currents at a given place and time.

Summary

A nearshore current modeling system has been assembled and used to hindcast the wave-driven component of longshore flow for two events at CERC's FRF where wave and current measurements are available. The modeling system is composed of a directional spectral wave model, an algorithm to calculate the components of radiation stress from the spectral wave model and a current model which uses the radiation stress components to calculate the nearshore wave-driven currents.

The first event hindcast was characterized by high winds and local wave generation. Measured longshore flow was relatively uniform in strength and direction from shore to the seaward most measurement station. The computed wave-driven component of flow was also relatively uniform in direction and speed, but only a fraction of the measured value. The discrepancy is attributed to processes other than wave-driven flow which were present but not modeled.

The second event was characterized by low winds and long period waves. The measured and hindcast longshore flow compare well in speed and direction indicating a condition of primarily wave-driven currents. Again, the longshore flow is generally uniform in speed and direction along the measurement profile.

The present nearshore current modeling system shows promise as a tool for studying and predicting nearshore current processes. Employing the directional spectral approach to specify the nearshore wave climate and radiation stress field appears to result in a more uniform cross-shore profile of longshore flow than a monochromatic approach. This is accomplished without resorting to lateral eddy viscosity or mixing parameters to smooth the profile. The more uniform profile is in agreement with the profiles measured at the FRF in October 1982.

A field measurement experiment to support nearshore wave and current model verification and to study nearshore processes is planned for the fall of 1986 at CERC's FRF. Interested investigators are invited to participate in the planning and execution of the experiment. A preliminary set of experiment objectives is available from the author.

Acknowledgments

I would like to acknowledge helpful discussions with Dr. Linwood Vincent on the wave model, Dr. Rao Vemulakonda on the current model and Dr. Abby Sallenger on the field measurements. This work was carried out under the Coastal Engineering Research Center's Nearshore Waves and Currents Work Unit, Harbor Entrances and Coastal Channels Program, Coastal Engineering Functional Area of Civil Works Research and Development. The author wishes to acknowledge the Office, Chief of Engineers, U. S. Army Corps of Engineers, for authorizing publication of this paper.

Appendix.-References

1. Basco, D.R., "Surfzone Currents," Coastal Engineering, Vol. 7, 1983, pp. 331-355.
2. Bouws, E., Gunther, H., Rosenthal, W., Vincent, C.L., "Similarity of the Wind Wave Spectrum in Finite Depth Water, Part 1 - Spectral Form," accepted for publication in the Journal of Geophysical Research, 1984.
3. Butler, H.L., "Evolution of a Numerical Model for Simulating Long Period Wave Behavior in Ocean-Estuarine Systems," Estuarine and Wetlands Processes with Emphasis on Modeling, Marine Sciences Series, Vol. 11, Plenum Press, New York, 1980.
4. Hasselmann, K., Ross, D.B., Muller, P., Sell, W., "A Parametrical Wave Prediction Model," Journal of Physical Oceanography, Vol 6, 1976, pp 201-228.
5. Hsiao, V., "On the Transformation Mechanisms and the Prediction of Finite -Depth Water Waves," Dissertation, University of Florida, 1978.
6. Kitaigorodskii, S.A., Krasitskii, V.P., Aaslavskii, M.M., "On Phillips' Theory of Equilibrium Range in the Spectra of Wind Tenerated Gravity Waves," Journal of Physical Oceanography, Vol. 5, 1975, pp 410-420.
7. Longuet-Higgins, M.S., Stewart, R.W., "Radiation Stresses in Water Waves: A Physical Discussion with Application," Deep Sea Research, Vol. 11, 1964, pp 529-562.
8. Vemulakonda, S.R., Houston, J.R., Butler, H.L., "Modeling Longshore Currents for Field Situations," Proceedings, 18th Conference on Coastal engineering, 1982, pp 1659-1676.